Magnetic field structure of OMC-3 in the far infrared revealed by SOFIA/HAWC+ (A&A 659, A22)

Niko Zielinski & Sebastian Wolf

SOFIA Community Tele-Talk Series

Institut für Theoretische Physik und Astrophysik
Christian-Albrechts-Universität zu Kiel

May 25, 2022

Magnetic fields

- Magnetic fields in astrophysical objects are ubiquitous and can be found on both small and large scales
- Impact of magnetic fields in various physical processes unknown
- Measure strength and structure of magnetic fields during individual stages of the star-formation process
  $\rightarrow$ polarimetric oberservations of the thermal reemission radiation (e.g., HAWC+ on SOFIA)

  $\rightarrow$ indirect measurement of the magnetic field

OMC-3

- Orion molecular cloud complex: massive star-formation
- OMC-3: part of the integral shape filament of the Orion molecular cloud
- Several prestellar and protostellar sources in OMC-3 (Chini et al. 1997)
- Well-studied region: polarimetric observations from far-infrared to mm wavelengths (Matthews et al. 2001; Houde et al. 2004; Takahashi et al. 2019; Liu et al. 2021)
- HAWC+: large-scale magnetic field structure & polarization spectrum of OMC-3

Polarization maps of OMC-3

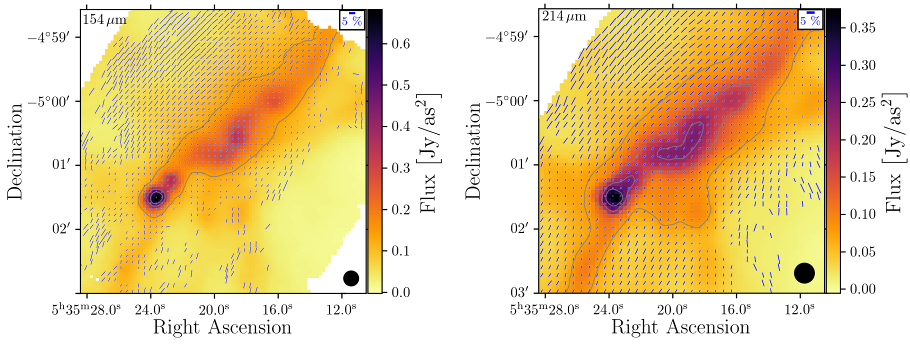

$$\frac{p}{\sigma_p} > 3, \qquad \frac{I}{\sigma_I} > 100 \tag{1}$$

Histogram polarization angle

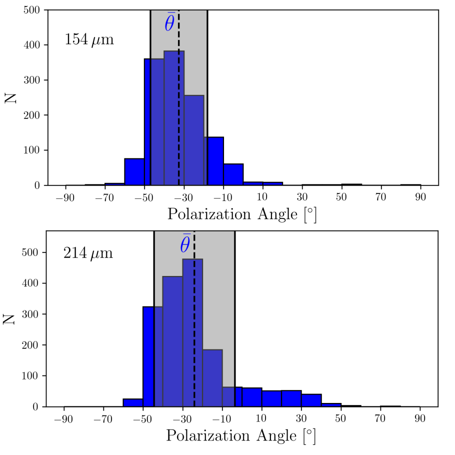

- High number of detections
- $\overline{\theta_{154\mu m}}$ = -32.6 $\pm$ 14.5°
- $\overline{\theta_{214\mu m}}$ = -24.1 $\pm$ 20.4°

Histogram polarization degree

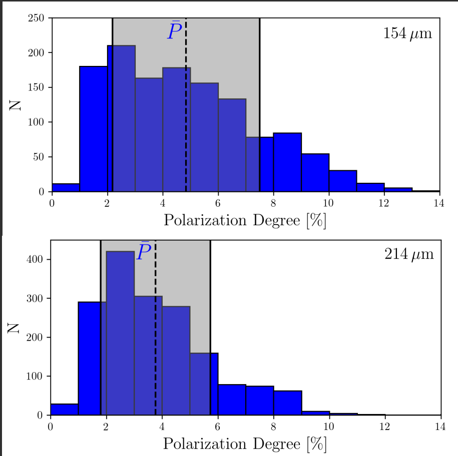

- $\overline{p_{154\mu\text{m}}} = 4.8 \pm 2.7\,\%$
- $\overline{p_{214\mu\text{m}}} = 3.8 \pm 2.0\,\%$
- $\overline{p_{154\mu\text{m},\, I > 0.2 \cdot I_{\text{max}}}}$ $= 2.3 \pm 1.0\,\%$
- $\overline{p_{214\mu\text{m},\, I > 0.2 \cdot I_{\text{max}}}}$ $= 2.5 \pm 1.0\,\%$

Origins of polarization

- Self-scattering (Kataoka et al. 2015)
- Supersonic mechanical grain alignment (Gold 1952)
- Mechanical alignment torques (MATs, Hoang et al. 2018)
- Dust grain alignment due to radiative torque alignment
  - B-RATs (e.g., Dolginov & Mitrofanov 1976; Lazarian & Hoang 2007)
  - k-RATs (e.g., Tazaki et al. 2017)

Magnetic field structure

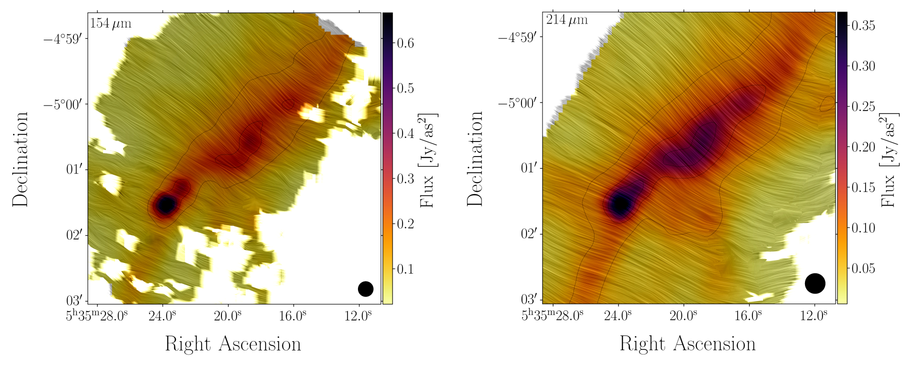

- Magnetic field is visualized using the line-integral-convolution technique (LIC, Cabral & Leedom 1993)
- Magnetic field direction is oriented perpendicular to the filament structure

Magnetic field strength

- Calculating magnetic field strength (Chandrasekhar & Fermi 1953)

$$B_{\mathsf{pos}} = Q\,\sqrt{4\pi\rho}\,\frac{\sigma_v}{\sigma_\theta} \approx 9.3\,\sqrt{n(\mathsf{H}_2)}\,\frac{\Delta v}{\sigma_\theta}\,\mu\mathsf{G}$$

$$B = \frac{4}{\pi}\,B_{\mathsf{pos}}$$

- B = 202 μG (154 μm) & B = 261 μG (214 μm)
  $\rightarrow$ similiar to literature values (190 μG, Poidevin et al. 2010)

- Mass-to-flux ratio (Crutcher et al. 2004):

$$\lambda = 7.6 \times 10^{-21}\,\frac{N(\mathsf{H}_2)}{B}\,\frac{\mu\mathsf{G}}{\mathsf{cm}^2} = \begin{cases} 0.64^{+0.10}_{-0.22} & \text{at } 154\,\mu\mathrm{m}, \\ 0.49^{+0.07}_{-0.15} & \text{at } 214\,\mu\mathrm{m} \end{cases} \quad (2)$$

Correlation between magnetic field structures and cloud properties

- Construct column density and temperature map of OMC-3 (following Santos et al. 2019; Chuss et al. 2019)

- Approach: Single-temperature modified blackbody fit:

$$I_\nu = (1 - \exp(-\tau_\nu))\, B_\nu(T)$$

- Optical depth

$$\tau_\nu = \epsilon\, (\nu/\nu_0)^\beta$$

$$\epsilon = \kappa_{\nu_0}\, \mu\, m_H\, N(H_2) \qquad \kappa_{\nu_0} = 0.1\,\mathrm{cm}^2\,\mathrm{g}^{-1} \quad \nu_0 = 1000\,\mathrm{GHz}$$

$$I_\nu = \left(1 - \exp\left(-\kappa_{\nu_0}\, \mu\, m_H\, N(H_2)\, (\nu/\nu_0)^\beta\right)\right)\, \frac{2h\,\nu^3}{c^2}\, \frac{1}{\exp\left(\frac{h\,\nu}{k\,T}\right) - 1}$$

Correlation between magnetic field structures and cloud properties

- Construct column density and temperature map of OMC-3 (following Santos et al. 2019; Chuss et al. 2019)
- Archival observations at 70 μm, 160 μm (*Herschel* PACS) and 850 μm (JCMT/SCUBA-2)
- Data preparation necessary:
  - re-projecting all to data to pixel scale of measurement at 214 μm
  - beam-convolving the 70, 154, 160, and 850 μm data to 18.2″ with kernel size $\sqrt{\mathrm{FWHM}_0^2 - \mathrm{FWHM}_{214\,\mu\mathrm{m}}^2}$

Correlation between magnetic field structures and cloud properties

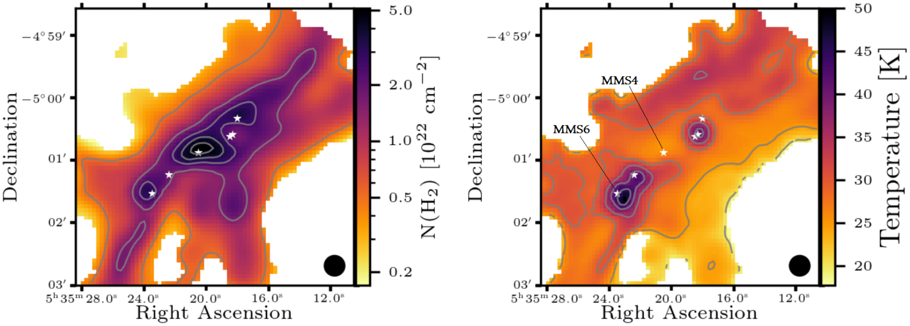

- "$\star$": known stellar sources (Chini et al. 1997)
- Position of stellar sources is closely connected to an increased temperature

Correlation between magnetic field structures and cloud properties

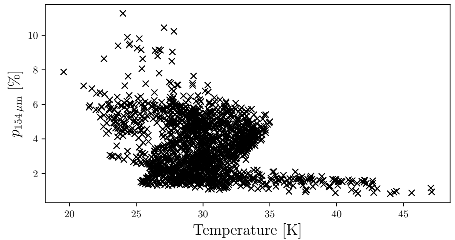

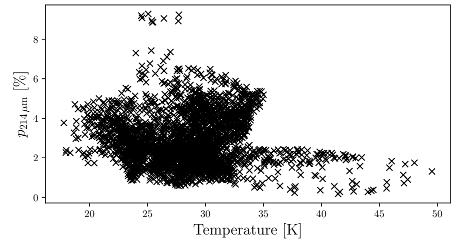

- $\overline{T} = 28\,\mathrm{K}$
- High temperature $\rightarrow$ low degree of polarization
- Low temperature $\rightarrow$ high degree of polarization

Correlation between magnetic field structures and cloud properties

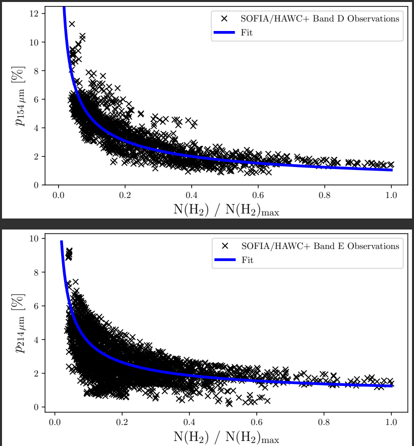

- Polarization degree decreases with column density
- Davis et al. (2000); Henning et al. (2001):

$$p = a_0 + a_1 \cdot \left(\frac{N(H_2)}{N(H_2)_{\mathrm{max}}} \right)^{a_2}$$

- a_2: Slope of the curve

Correlation between magnetic field structures and cloud properties

- Compare a_2 to literature values:

Object	Wavelength	Instrument	$\mathbf{a_2}$	Reference
OMC-3	154 μm	SOFIA/HAWC+	-0.51	this paper
OMC-3	214 μm	SOFIA/HAWC+	-0.63	this paper
B335	214 μm	SOFIA/HAWC+	-0.55	Zielinski et al. (2021)
B335	850 μm	JCMT/SCUBA	-0.43	Wolf et al. (2003)
CB54	850 μm	JCMT/SCUBA	-0.64	Henning et al. (2001)
DC 253-1.6	850 μm	JCMT/SCUBA	-0.55	Henning et al. (2001)

- Similar values $\rightarrow$ Occurence of the same underlying mechanism(s)?

Possible origins of de-polarization

- Increased disalignment of the dust grains towards core due to higher density and temperature (Goodman et al. 1992)
- Insufficient angular resolution of a possibly complex magnetic field structure on scales below the resolution of the polarization maps (Shu et al. 1987)
- Less elongated dust grains in dense regions (e.g., Creese et al. 1995; Goodman et al. 1995)
- Unaligned graphite grains accumulated in dense regions (e.g., Hildebrand et al. 1999)
- Disruption of spinning large dust grains into smaller fragments (radiative torque disruption, Hoang et al. 2019)
- Polarized emission vs. dichroic absorption (Brauer et al. 2016)

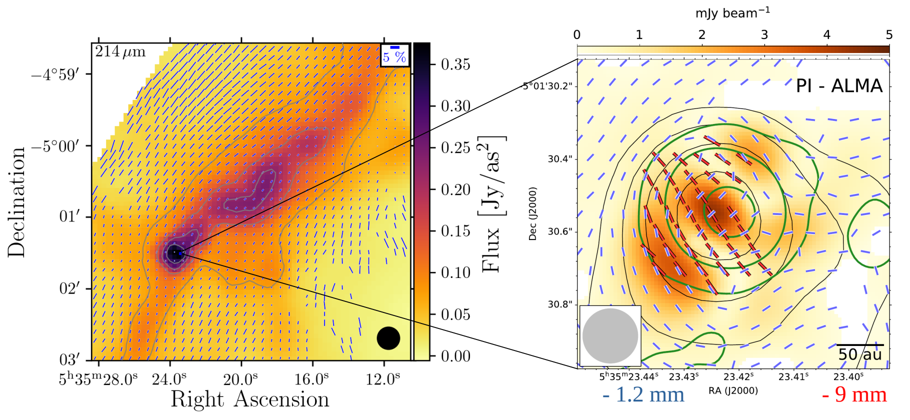

- Comparison: 1.2 mm ALMA & 9 mm JVLA (Liu 2021) → 90° flip
- Magnetic field in OMC-3 is more complex on smaller scales

Polarization spectrum

- Polarization spectrum: polarization degree as a function of wavelength
- First measured in the far-infrared by Hildebrand et al. (1999) using the Kuiper Airborne Observatory
- SOFIA/HAWC+: higher angular resolution and sensitivity
- 'Typical' definition:

  $p_{214\,\mu\mathrm{m}}/p_{154\,\mu\mathrm{m}} < 1$: negative spectral slope
  $p_{214\,\mu\mathrm{m}}/p_{154\,\mu\mathrm{m}} > 1$: positive spectral slope

Polarization spectrum map of OMC-3

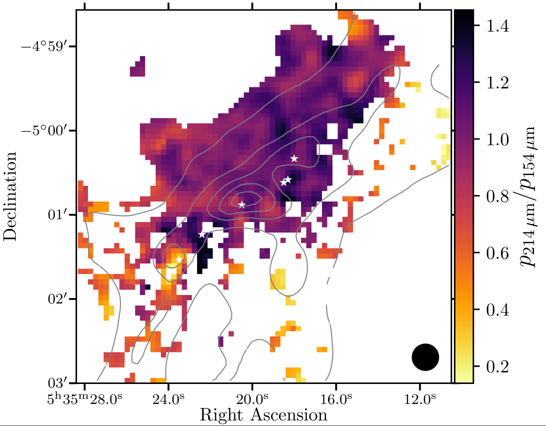

- southern and eastern part: $p_{214\,\mu\mathrm{m}}/p_{154\,\mu\mathrm{m}} < 1$,
- central and northern part: $p_{214\,\mu\mathrm{m}}/p_{154\,\mu\mathrm{m}} > 1$
- $\overline{p_{214\,\mu\mathrm{m}}/p_{154\,\mu\mathrm{m}}} = 0.93 \pm 0.24$

Polarization spectrum versus column density and temperature

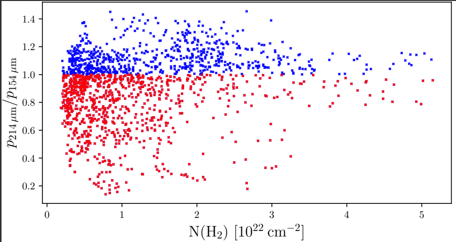

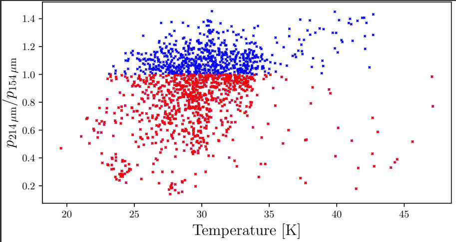

- polarization spectrum flat (∼1) at higher column densities
- polarization spectrum negative (<1) for low and high temperatures
- no correlation between polarization spectrum and cloud properties

Magnetic field of OMC-3 derived from observations in different wavelength ranges

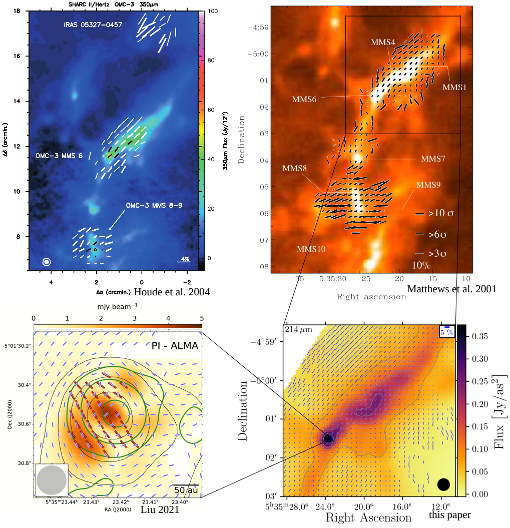

- magnetic field: uniform at larger scales, greater level of complexity on small scales
- de-polarization at 350 μm not as prominent as at 154, 214, 850 μm (MMS6)

Summary

- Investigated the magnetic field of OMC-3 with SOFIA/HAWC+ at 154 and 214 μm
- Mean polarization angles: $\theta_{154\,\mu\mathrm{m}} =$ -32.6 $\pm$ 14.5°
  $\theta_{214\,\mu\mathrm{m}} =$ -24.1 $\pm$ 20.4°
- Polarization degree decreases for both wavelengths toward regions with increased column density
- No general correlation between the polarization spectrum and column density $N(H_2)$ or temperature T
- Derived magnetic field structure consistent with previous observations at far-infared and sub-mm wavelengths

Brauer, R., Wolf, S., & Reissl, S. 2016, Astronomy & Astrophysics, 588, A129

Cabral, B. & Leedom, L. C. 1993, in Proceedings of the 20th annual conference on Computer graphics and interactive techniques, SIGGRAPH '93 (New York, NY, USA: ACM), 263–270

Chandrasekhar, S. & Fermi, E. 1953, ApJ, 118, 116

Chini, R., Reipurth, B., Ward-Thompson, D., et al. 1997, The Astrophysical Journal, 474, L135

Chuss, D. T., Andersson, B. G., Bally, J., et al. 2019, ApJ, 872, 187

Creese, M., Jones, T. J., & Kobulnicky, H. A. 1995, AJ, 110, 268

Crutcher, R. M., Nutter, D. J., Ward-Thompson, D., & Kirk, J. M. 2004, ApJ, 600, 279

Davis, C. J., Chrysostomou, A., Matthews, H. E., Jenness, T., & Ray, T. P. 2000, ApJL, 530, L115

Dolginov, A. Z. & Mitrofanov, I. G. 1976, APSS, 43, 291

Gold, T. 1952, Monthly Notices of the Royal Astronomical Society, 112, 215

Goodman, A. A., Jones, T. J., Lada, E. A., & Myers, P. C. 1992, ApJ, 399, 108

Goodman, A. A., Jones, T. J., Lada, E. A., & Myers, P. C. 1995, ApJ, 448, 748

Henning, T., Wolf, S., Launhardt, R., & Waters, R. 2001, ApJ, 561, 871

Hildebrand, R. H., Dotson, J. L., Dowell, C. D., Schleuning, D. A., & Vaillancourt, J. E. 1999, ApJ, 516, 834

Hoang, T., Cho, J., & Lazarian, A. 2018, ApJ, 852, 129

Hoang, T., Tram, L. N., Lee, H., & Ahn, S.-H. 2019, Nature Astronomy, 3, 766

Houde, M., Dowell, C. D., Hildebrand, R. H., et al. 2004, ApJ, 604, 717

Kataoka, A., Muto, T., Momose, M., et al. 2015, ApJ, 809, 78

Lazarian, A. & Hoang, T. 2007, MNRAS, 378, 910

Liu, H. B. 2021, ApJ, 914, 25

Liu, J., Qiu, K., & Zhang, Q. 2021, arXiv e-prints, arXiv:2111.05836

Matthews, B. C., Wilson, C. D., & Fiege, J. D. 2001, ApJ, 562, 400

Poidevin, F., Bastien, P., & Matthews, B. C. 2010, ApJ, 716, 893

Santos, F. P., Chuss, D. T., Dowell, C. D., et al. 2019, ApJ, 882, 113

Shu, F. H., Adams, F. C., & Lizano, S. 1987, ARA&A, 25, 23

Takahashi, S., Machida, M. N., Tomisaka, K., et al. 2019, ApJ, 872, 70

Tazaki, R., Lazarian, A., & Nomura, H. 2017, ApJ, 839, 56

Wolf, S., Launhardt, R., & Henning, T. 2003, The Astrophysical Journal, 592, 233

Zielinski, N., Wolf, S., & Brunngräber, R. 2021, A&A, 645, A125